JOURNAL OF GEOPHYSICAL RESEARCH: EARTH SURFACE, VOL. 118, 2159–2173, doi:10.1002/jgrf.20147, 2013

Evaluation of a gully headcut retreat model using multitemporal aerial photographs and digital elevation models

M. A. Campo-Bescós,[1] J. H. Flores-Cervantes,[2] R. L. Bras,[3]
J. Casalí,[1] and J. V. Giráldez[4]

Received 9 November 2012; revised 4 September 2013; accepted 17 September 2013; published 16 October 2013.

[1] A large fraction of soil erosion in temperate climate systems proceeds from gully headcut growth processes. Nevertheless, headcut retreat is not well understood. Few erosion models include gully headcut growth processes, and none of the existing headcut retreat models have been tested against long-term retreat rate estimates. In this work the headcut retreat resulting from plunge pool erosion in the Channel Hillslope Integrated Landscape Development (CHILD) model is calibrated and compared to long-term evolution measurements of six gullies at the Bardenas Reales, northeast Spain. The headcut retreat module of CHILD was calibrated by adjusting the shape factor parameter to fit the observed retreat and volumetric soil loss of one gully during a 36 year period, using reported and collected field data to parameterize the rest of the model. To test the calibrated model, estimates by CHILD were compared to observations of headcut retreat from five other neighboring gullies. The differences in volumetric soil loss rates between the simulations and observations were less than 0.05 $m^3\ yr^{-1}$, on average, with standard deviations smaller than 0.35 $m^3\ yr^{-1}$. These results are the first evaluation of the headcut retreat module implemented in CHILD with a field data set. These results also show the usefulness of the model as a tool for simulating long-term volumetric gully evolution due to plunge pool erosion.

Citation: Campo-Bescós, M. A., J. H. Flores-Cervantes, R. L. Bras, J. Casalí, and J. V. Giráldez (2013), Evaluation of a gully headcut retreat model using multitemporal aerial photographs and digital elevation models, *J. Geophys. Res. Earth Surf.*, *118*, 2159–2173, doi:10.1002/jgrf.20147.

1. Introduction

[2] Gully erosion is a natural and important soil loss process [e.g., *De Ploey*, 1990; *Poesen et al.*, 2003; *Valentin et al.*, 2005] that causes great damage to the environment [*Poesen et al.*, 2003] and to infrastructure [*Powledge et al.*, 1989; *Moore et al.*, 1994; *Temple and Hanson*, 1994; *Wahl*, 1998; *Hanson et al.*, 2001]. Gully erosion can be considered the most important source of sediment production in the Mediterranean landscape [e.g., *Martínez-Casasnovas et al.*, 2003; *Poesen et al.*, 2003; *De Santisteban et al.*, 2006].

[3] Gully erosion is defined as the soil loss and sediment yield generated by water runoff carving the headcut pool and downstream channels, followed by the slide or collapse of the borders and the subsequent removal of the deposited soil. Two types of gullies are described in the literature: permanent and ephemeral gullies. Permanent gullies are often associated with agricultural land and are caused by the concentrated but intermittent flow of water usually during and immediately following heavy rain, with the flow being deep enough to interfere with, and not to be obliterated by, normal tillage operations. These gullies typically range from 0.5 m to as much as 25 to 30 m in depth [*Soil Science Society of America* (*SSSA*), 2001]. Permanent gullies are typically found in abandoned agricultural fields, rangelands, or shrubland [*Poesen et al.*, 2002]. Several definitions of ephemeral gullies have been given in the literature. According to the *SSSA* [2001], ephemeral gullies are small channels that are eroded by concentrated flow and subsequently, filled by normal tillage, only to reform again in the same location by later runoff events.

[4] The causes, processes, prediction, and control of gully erosion have aroused the interest of many researchers in different environments. Most research has analyzed gully morphology and its development stages as a first step in evaluating these processes, assessing its potential erosion [e.g., *Ireland et al.*, 1939; *Heede*, 1976]. *Sidorchuk* [1999] described two main developmental stages of gully evolution: active and stable. During the active gully stage, erosion is intense and the associated morphological characteristics (e.g., width, depth, slope, etc.) are variable. This active growth

[1]Department of Projects and Rural Engineering, Universidad Pública de Navarra, Pamplona, Spain.
[2]Department of Civil and Environmental Engineering, University of Washington, Seattle, Washington, USA.
[3]School of Civil and Environmental Engineering and School of Earth and Planetary Sciences, Georgia Institute of Technology, Atlanta, Georgia, USA.
[4]Department of Agronomy, Universidad de Cordoba, Cordoba, Spain.

Corresponding author: M. A. Campo-Bescós, Department of Projects and Rural Engineering, Universidad Pública de Navarra, ES-31006 Pamplona, Spain. (miguel.campo@unavarra.es)

2169-9003/13/10.1002/jgrf.20147

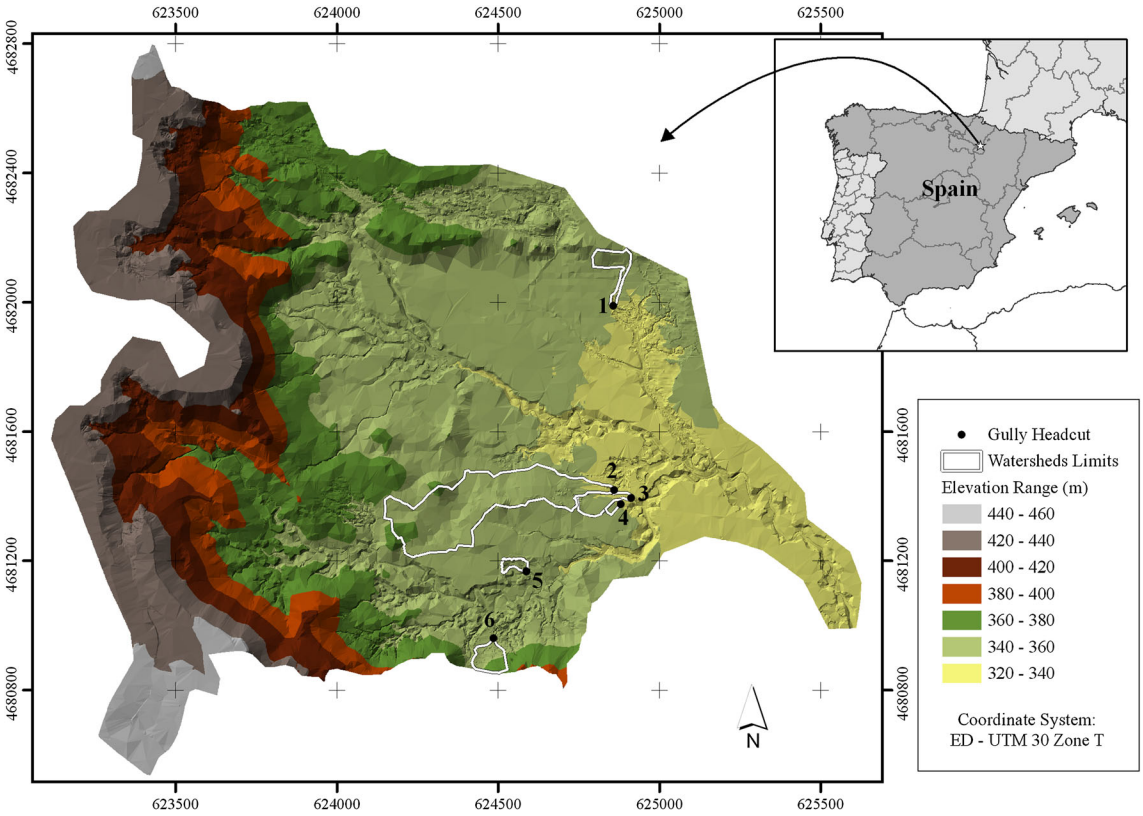

Figure 1. Location of El Cantalar watershed and gully headcuts used for this study (black dots). Gully 1 was selected for calibration and gullies 2 to 6 for validation. The watershed limit for each gully is shown (white line).

stage is governed by three processes: retreat of the headcut upstream, channel bed incision, and widening of the channel cross section. In semiarid environments, gully headcut retreat is one of the main driving processes of its growth [*Rieke-Zapp and Nichols*, 2011]. *Oostwoud Wijdenes and Bryan* [1994] reported that headcut retreat was the main source of sediment in a semiarid part of Kenya. Similar results were found by *Oostwoud Wijdenes et al*. [2000] and *Vandekerckhove et al*. [2001, 2003] in southeastern Spain. Within the Ebro Valley, northeast Spain, gullying is a characteristic and widespread phenomenon in the landscape [e.g., *Casalí et al*., 1999; *Ries and Marzolff*, 2003; *Gimenez et al*., 2009]. Two main processes are presented as the main drivers of gully headcut retreat: piping and falling water at the gully base, described as plunge pool erosion [*Del Valle De Lersundi and Del Val*, 1990; *Seeger et al*., 2009].

[5] Gully headcut retreat has been modeled in two different ways. A first approach uses statistical relationships based on combinations of environmental variables (e.g., rainfall, flow discharge, topography, soil properties, and land use) [e.g., *Thompson*, 1964; *Seginer*, 1966; *Vandekerckhove et al*., 2003; *Capra et al*., 2009; *Nazari Samani et al*., 2010]. However, processes behind these relationships are scantily explained. Another approach is through conceptual or physically based modeling, where mathematical relationships based upon the balance between erosive forces and resistance of the local surface explain the gully headcut retreat process. Based on slope stability, *Bradford and Piest* [1980] modeled headcut retreat under mass wasting or slab failure. *Howard and MacLane* [1988] and *Lobkovsky et al*. [2007] analyzed erosion of soils on noncohesive soils caused by groundwater seepage. Gully headcut retreat due to the formation of plunge pools was conceptualized by *De Ploey* [1989]. Later, *Alonso et al*. [2002] presented a physical model to describe gully headcut retreat due to plunge pool erosion, which was validated by available experimental data collected by *Robinson* [1989], *Bennett* [1999], *Bennett et al*. [2000] and *Bennett and Casalí* [2001]. However this approach has not been evaluated with three-dimensional long-term data from permanent gullies [*Valentin et al*., 2005].

[6] There are few landscape evolution models that include gully processes [*Coulthard*, 2001]. Specifically, there are only two models that address gully evolution due to headcut retreat: AnnAGNPS (Agricultural Nonpoint Source Pollution Model) [*Bingner et al*., 2009] and CHILD (Channel Hillslope Integrated Landscape Development) [*Flores-Cervantes et al*., 2006]. Both models address gully evolution due to headcut retreat based upon the model of *Alonso et al*. [2002]. AnnAGNPS simulates multiple ephemeral gullies on a cultivated planar surface [*Bingner et al*., 2009]. The ephemeral gully headcut is located through the use of topographic indices [*Momm et al*., 2012] or defined by the user. The maximum gully length is a function of the given drainage area [*Leopold et al*., 1964]. The channel width is changed using a stream power relation based on discharge [*Nachtergaele et al*., 2002] or in combination with slope [*Wells et al*., 2013]. A version of CHILD [*Flores-Cervantes et al*., 2006] simulates the evolution of multiple bifurcating permanent

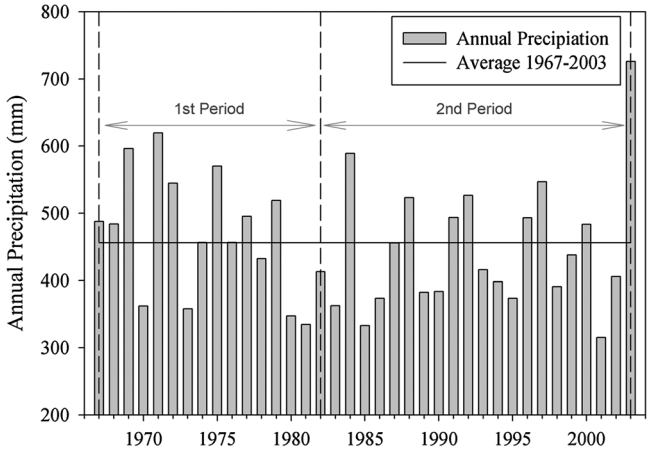

Figure 2. Annual precipitation registered at Carcastillo station from 1967 to 2003 (vertical bar) and average annual precipitation (solid black). First studied period from 1967 to 1982 and second period from 1982 to 2003.

gullies resulting from plunge pool erosion. In this case, the gully headcut is located based on a digital elevation model (DEM) filter [*Flores-Cervantes et al*., 2006]. The gully grows until the shear stress of the erosive flow is lower than the soil resistance or until the topographical gully headcut condition disappears. Then the gully headcut location is modeled as classical bed fluvial erosion or stream erosion. CHILD changes the topographic elevation through time, while AnnAGNPS keeps the landscape constant. In addition, CHILD includes a slab failure component for widening of the channel cross section [*Istanbulluoglu et al*., 2005].

[7] The lack of detailed field data about gully evolution due to plunge pool retreat, particularly of permanent gullies, is an obstacle for model evaluation [*Valentin et al*., 2005]. However, several studies have used field or experimental data to evaluate models. *Gordon et al*. [2007] used AnnAGNPS to compare measured and simulated dimensions of ephemeral gullies at four agricultural field sites in central Mississippi using field data reported by *Smith* [1992] for single storm events. They found a reasonably good prediction of lengths but a less favorable prediction of widths. The aforementioned investigation dealt with the position and size of ephemeral gullies in one agricultural year. *Gordon et al*. [2008] used data from Belgium, Mississippi, Iowa, and Georgia to simulate a continuous 10 year period of ephemeral gully development under conditions of till and no till. When agricultural fields were not tilled annually, their study suggested that gullies attain their maximum dimensions during the first few years in response to several relatively large runoff events. The modeled erosion rates in these four geographic regions were 250% to 450% greater when gullies were tilled and reactivated annually than in the absence of any tillage. However, at present, long-term field data have not been used to test the model of *Alonso et al*. [2002] or its implementation in the landscape evolution model CHILD.

[8] This paper presents the results of a 36 year study of six gully headcuts in a watershed within the Ebro Valley in Spain, which were caused by plunge pool erosion. The effort uses a combination of multitemporal aerial photographs to infer gully evolution at the site and the CHILD model with a gully retreat module. We chose this model because (1) the model was designed to test different geomorphological processes, (2) the model allows changes on landscape elevation, and (3) the model had not been evaluated under field conditions. Our main objective is to analyze the long-term dynamics of permanent gullies due to plunge pool and evaluate the headcut retreat module implemented in CHILD.

2. Study Area

[9] The Bardenas Reales Natural Park (Navarra, Spain), a World Biosphere Reserve, is located in the central sector of the Tertiary Ebro Basin, northeastern Spain. In the erosive depression of the northern sector of Bardenas Reales, a 300 ha semiarid watershed named El Cantalar was selected for this study (Figure 1). El Cantalar was chosen due to the presence of several gullies of different sizes and morphologies (e.g., width, depth, slope, developed over homogenous soil profile, and limited by bed rock), which are representative of many parts of the central sector of the Ebro Basin [e.g., *Casalí et al*., 1999; *Martínez-Casasnovas et al*., 2003; *Ries and Marzolff*, 2003; *De Santisteban et al*., 2005].

[10] El Cantalar was formed by incision and erosion mechanisms triggered by downcutting in the Ebro and Aragón Rivers [*Sancho et al*., 2008]. Bedrock is composed mainly of horizontal claystones-siltstones with beds of gypsum, sandstones, and limestones and is Miocene in age [*Larrasoaña et al*., 2006]. More recent Quaternary fluvial aggradational phases are evident in river terraces and cover pediments. The watershed has a flattened bottom, located around 340 m above sea level, overlain by several upper Pleistocene-Holocene alluvial morphosedimentary units originating from the erosion of surrounding clayey Tertiary bedrock [*Sancho et al*., 2008].

[11] This region is characterized by a semiarid climate with strong seasonality. The mean annual temperature is 14°C, with a mean minimum value of 5.4°C in January and a mean maximum value of 24°C in July, based on the information of the weather station of Carcastillo, located 10 km away from the site, during the period 1967–2003. Mean annual precipitation is 456 mm (Figure 2) and the standard deviation is 93 mm. Monthly precipitation distribution is bimodal, with wet periods in April–June and September–October. These periods produce around 70% of the total annual precipitation.

[12] Based on visual inspection in 2007, six gullies from El Cantalar were selected for this study (Figure 3). These gullies have a headcut with a plunge pool developed in a homogeneous soil profile, without any layer of bedrock. The gullies had a marked flow path upstream of the overfall, which drives the direction of retreat. There were no signs of piping processes in the vicinity of the headcut, even though these processes might have occurred in earlier stages. Based on such an absence of piping processes, we surmised that plunge pool erosion was the main headcut retreat process for these selected gullies. The main geometric properties of each gully were measured with a measuring tape, and samples of the soil profiles were collected at the site in 2007. Headcut heights ranged between 1.2 m and 2.7 m and widths ranged between 2.0 m and 3.8 m (see Table 1). Data for cross sections were averaged from three measurements located between 1 and 3 m downstream of the gully headcut. However, it is worth noting that eroding soil volume was estimated in a different way and is described in a following section. Based on the pipette method [*Day*, 1965], particle size analyses of the first 0.3 m of the soil

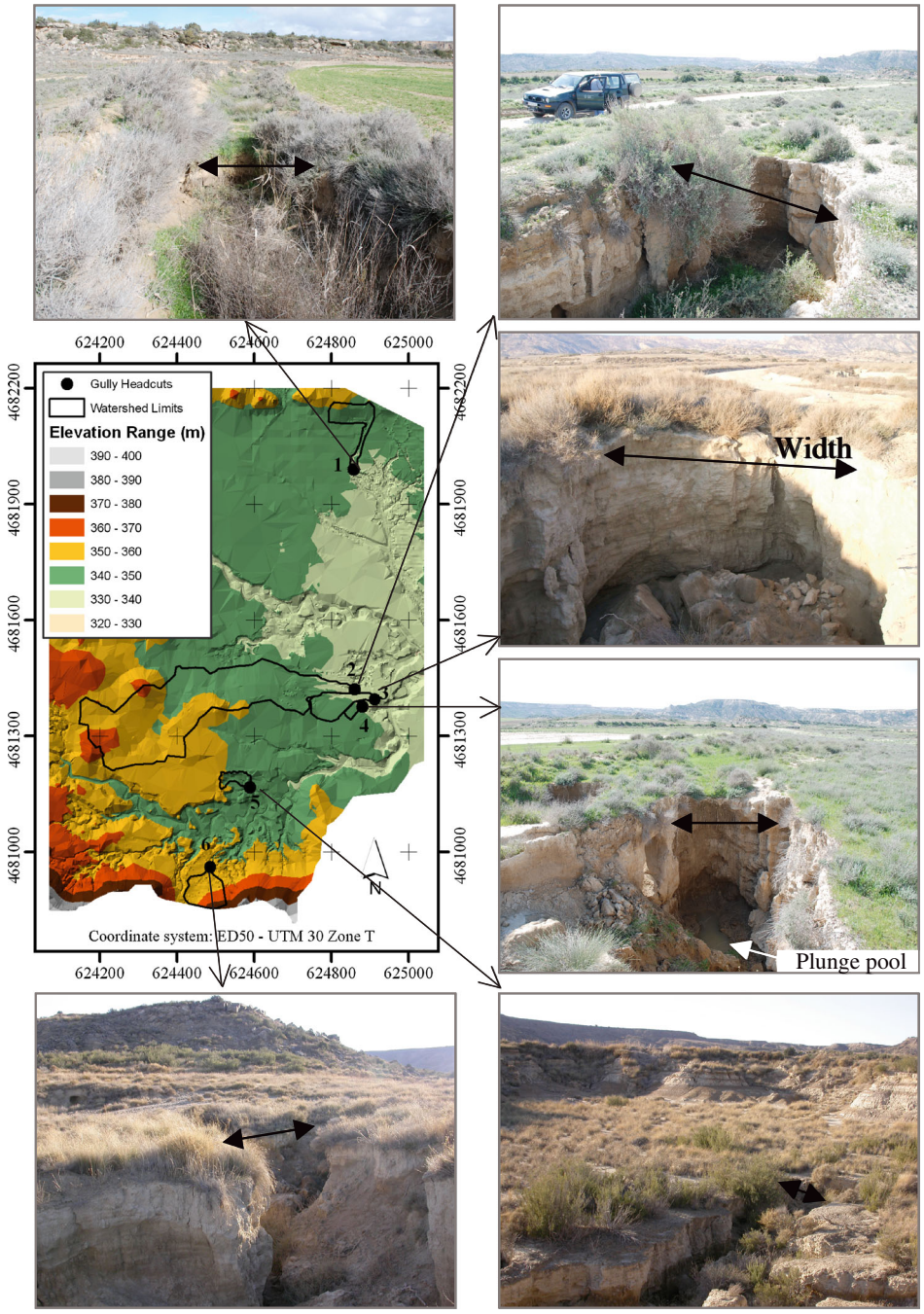

Figure 3. TIN from the 1967 data set, with watershed positions and photographs taken in 2007 of each headcut used.

profile at the top and base of the headcut ($n = 15$) indicate a high content of silt and clay, with a mean value of sand, silt, and clay of: 7%, 68%, and 25%, respectively. Gravel fraction was not detectable. The average bulk density was 1.4 ± 0.11 Mg m^{-3} ($n = 15$), based on ring samples 0.05 m in diameter at the top and base of the headcut [*Grossman and Reinsch*, 2002].

[13] Contributing area at the gully heads and land use were estimated using DEMs and orthophotographs, following the methods described in *Campo et al*. [2006]. The contributing areas ranged between 0.12 ha and 8.51 ha at the beginning of the observation period (Table 1). Scrubland predominates in the upstream areas of the gullies, except for gullies 3 and 4, where cropland is the dominant land use. Land use (Table 1) has not changed throughout the last century, due to the environmental policy of the Spanish Natural Park Administration.

3. Methods

3.1. Retreat Rates

[14] The long-term three-dimensional evolution of these gullies was calculated from multitemporal aerial photographic stereo pairs from 1967 (1:17,500 scale), 1982 (1:13,500), and 2003 (1:20,000), following the approach proposed by *Derose*

Table 1. Main Morphologic Characteristics of Gully Headcuts and Watersheds

	Headcut Characteristics (2003)				Contributing Area (1967)		
Gully	Depth	Width (m)	Shape Factor[a]	Textural Class (0–0.3 m) [b]	Area (ha)	Average Slope	Cropland Fraction
1	1.2	2.0	0.4	Silt loam	0.74	0.12	0.00
2	2.3	3.7	0.2	Silt loam	8.51[d]	0.10	0.25
3	2.2	3.5	0.4	Silty clay loam	0.73	0.04	0.62
4	2.7	2.6	0.3	Silty clay loam	0.12	0.06	0.54
5	1.2	2.4	0.5	Silt loam	0.25	0.25	0.04
6	2.1	3.8	[c]	Silt loam	0.78	0.22	0.45

[a]The shape factor is the ratio of pool's depth to the pool's midlength (see Figure 4).
[b]Texture class based on soil texture ternary diagram with clay, silt, and sand defined as grains <2 μm, grains 2–50 μm, and grains >2000 μm, respectively.
[c]It was filled by a bank failure and it was not possible to measure.
[d]In 2003, it was 0.85 ha.

et al. [1998], *Nachtergaele and Poesen* [1999], *Daba et al*. [2003], *Martínez-Casasnovas* [2003], *Hapke* [2005], and *Rieke-Zapp and Nichols* [2011]. Three-dimensional coordinates of contour lines and discontinuities in the topographic surface (e.g., cliffs, drainage lines, and gully edges) were obtained by photogrammetric processes from the stereo pairs [*Wolf and Dewitt*, 2000]. The process consists of building up a three-dimensional model from aerial photographic images by visual interpretation. This data manipulation was carried out by experts from TRACASA, a Spanish public company. The digital stereoscopic plotting instrument used the Digi3D.NET software package (Digi21 Ltd., Madrid, Spain). The geometric transformation in every restitution of the aerial photographic material produced a root-mean-square error less than 0.13 m in both x and y directions and less than 0.19 m in z (elevation). TINs (triangular irregular networks) were prepared for each year (see Figure 1 and 3) using a triangular interpolation scheme implemented in ArcGIS (ESRI™). Next, the TINs were interpolated to 2 m resolution DEMs (digital elevation models). This resolution was selected based on the concept that grid resolution should be at most half the average spacing between the closest point pairs used in the TIN [*Hengl*, 2006], or, in this case, points for each restitution.

[15] Based on the break lines, the linear gully headcut retreat rates were estimated (Table 2) for two time periods, 1967–1982 and 1982–2003. For each period analyzed, the measured error on linear gully headcut retreat was calculated by adding the restitution error of each aerial photogram used. The retreat rate of gully 2 decreased during the second period due to the construction of a spillway (ditch) upstream of the gully in the 1990s, which modified the stream pathway and drastically reduced the contributing area to 0.85 ha (a decrease of 90%). The precise date of construction is unknown.

Table 2. Measured and Simulated by CHILD Linear and Volumetric Retreat Rates of Gully Headcuts for the Different Time Periods[a]

	Gully Headcut							
	1	2	3	4	5	6	Mean[b]	SD[b]
				Linear Retreat (m/yr)				
1967–1982	0.74	1.80	0.48	0.07	0.10	0.21		
	±0.02	±0.02	±0.02	±0.02	±0.02	±0.02	0.32	0.29
	0.76	*4.01*	*0.86*	*0.07*	*0.12*	*0.80*	*0.52*	*0.39*
	±0.01	*±0.04*	*±0.01*	*±0.00*	*±0.00*	*±0.01*		
1982–2003	0.78	0.34	0.53	0.12	0.12	0.48		
	±0.01	±0.01	±0.01	±0.01	±0.01	±0.01	0.41	0.28
	0.73		*0.82*	*0.07*	*0.11*	*0.55*	*0.46*	*0.35*
	±0.01		*±0.01*	*±0.00*	*±0.00*	*±0.01*		
1967–2003	0.76		0.51	0.10	0.11	0.37		
	±0.01		±0.01	±0.01	±0.01	±0.01	0.37	0.28
	0.74		*0.84*	*0.07*	*0.12*	*0.65*	*0.48*	*0.36*
	±0.01		*±0.01*	*±0.00*	*±0.00*	*±0.01*		
				Volumetric Retreat (m^3/yr)				
1967–1982	1.76	15.36	3.67	0.53	0.29	1.68		
	±0.21	±2.93	±0.41	±0.62	±0.22	±0.24	1.59	1.34
	1.85	*15.41*	*4.84*	*0.34*	*0.26*	*3.76*	*2.21*	*2.05*
	±0.02	*±0.18*	*±0.05*	*±0.01*	*±0.01*	*±0.03*		
1982–2003	1.87	2.89	4.05	0.87	0.34	3.85		
	±0.23	±0.91	±0.57	±0.09	±0.30	±0.29	2.20	1.69
	1.81		*3.90*	*0.34*	*0.24*	*2.41*	*1.74*	*1.53*
	±0.01		*±0.03*	*±0.01*	*±0.01*	*±0.03*		
1967–2003	1.83	8.03	3.89	0.73	0.32	2.96		
	±0.22	±1.74	±0.51	±0.31	±0.27	±0.27	1.95	1.50
	1.83		*4.29*	*0.34*	*0.25*	*2.96*	*1.93*	*1.73*
	±0.01		*±0.02*	*±0.01*	*±0.00*	*±0.02*		

[a]Measured error and twice the standard deviation on 500 simulations below each respective value. Measured values are in roman and simulated ones are in italics.
[b]Calculated values without considering gully 2.

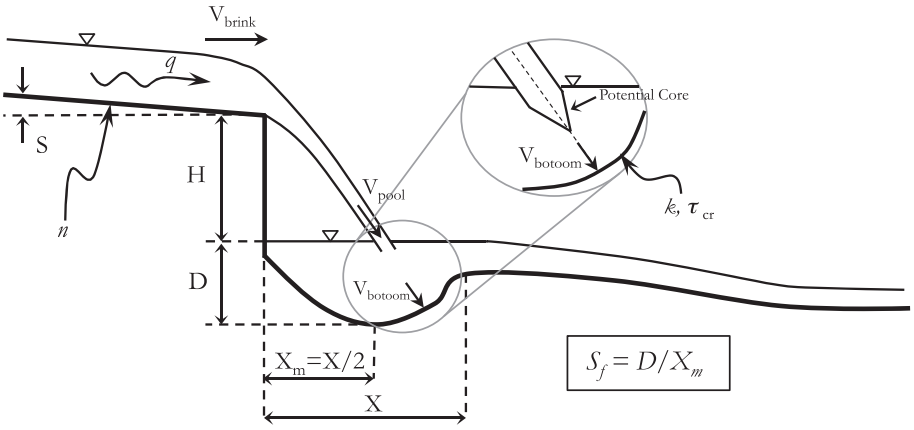

Figure 4. Sketch of the headcut-plunge-pool system.

Therefore, the second period of this gully was not modeled and the results of gully 2 will only focus on the first period.

[16] Volumetric headcut retreat rates for each period were calculated as the product of the linear retreat and a representative cross-section of each gully and period, both measures estimated from the manually restituted orthophotographs, following the methodologies previously proposed [e.g., *Vandaele et al*., 1996; *Vandekerckhove et al*., 2001, 2003; *Tebebu et al*., 2010]. Methods that estimate retreat rates based on DEMs [e.g., *Derose et al*., 1998; *Martínez-Casasnovas*, 2003] were not used because the resolution of both the DEMs and gully width monitoring data was similar. The representative cross-section for each gully was calculated based on restituted break lines in areas of extension since the earliest photo and on 10 cross-section measures for each gully headcut. Following *Nachtergaele and Poesen* [1999], a reasonable upper and lower volumetric limit for each headcut retreat was estimated based on the standard deviation of cross sections and linear retreat error.

3.2. Model Description

[17] CHILD is a computational framework that simulates the evolution of a three-dimensional topographic landscape driven by a number of erosion and sedimentation processes, given a set of initial and boundary conditions [*Tucker et al*., 2001a]. Topography is discretized as a set of points connected to form a triangulated irregular mesh, in which each node in the triangulation is associated with a Voronoi polygon. This spatial framework is an optimal computational way to represent the topographic surface [*Braun and Sambridge*, 1997; *Tucker et al*., 2001b]. In this study, elevation data (point) are provided in a regular grid (DEM from 1967). Watershed delineation follows the algorithm implemented by *Tucker et al*. [2001b]. Each Voronoi polygon is treated as a finite-volume cell. Changes in elevation are due to fluvial erosion and horizontal motion of a discrete gully headcut.

[18] CHILD can be modified and adapted to different studies. In this study in particular, fluvial erosion is assumed to be detachment-limited because we assume that any sediment detached from the surface is transported downstream and out of the system. Usually, upper watershed areas have little or no deposition of sediments [e.g., *Howard*, 1994]. The capacity of the flow to detach sediments for each node in the downstream direction is given by the following semiempirical equation [*Whipple and Tucker*, 1999]:

$$\frac{\partial z}{\partial t} = k\left(\rho g n^{0.6} q^{0.6} S^{0.7} - \tau_{cr}\right)^{p}, \tag{1}$$

where k is soil erodibility ($m^3\,N^{-1}\,yr^{-1}$), ρ is water density ($kg\,m^{-3}$), g is gravitational acceleration ($m\,s^{-2}$), n is Manning's roughness coefficient ($m^{-1/3}\,s$), q is discharge per unit width ($m^2\,s^{-1}$), S is bed slope ($m\,m^{-1}$), τ_{cr} is the critical shear stress (Pa), and p is an empirical coefficient. Note that the first term in parentheses represents flow shear stress, so detachment rate scales with excess shear stress. In this study, channel width is assumed to be equal to the Voronoi cell width, c [*Flores-Cervantes et al*., 2006]. The instantaneous discharge from each Voronoi cell in the watershed is the product of precipitation and drainage area. In this study, we neglect infiltration because soils have a low infiltration rate (silty soils that crust under heavy rainfall) and because erosion in these landscapes is driven by high-intensity events [*Poesen et al*., 2002], where infiltration plays a small role.

[19] The gully headcut retreat module implemented in CHILD [*Flores-Cervantes et al*., 2006] is based on algorithms inferred from experimental studies in flumes [*Stein and Julien*, 1993; 1994; *Stein et al*., 1993; *Bennett et al*., 2000; *Bennett and Casalí*, 2001; *Dey et al*., 2001; *Bennett and Alonso*, 2005] and developed by *Alonso et al*. [2002]. The model calculates the retreat rate of a headcut $\frac{dL}{dt}$ as a function of the rate of vertical deepening of the plunge pool $\frac{dD}{dt}$, divided by a shape factor S_f, as [*Flores-Cervantes et al*., 2006]

$$\frac{dL}{dt} = \frac{1}{S_f}\frac{dD}{dt}, \tag{2}$$

where L is the horizontal retreat length (m). The shape factor is the ratio of depth D (m) to the pool's mid length X_m (m), $S_f = D/X_m$, which is assumed to remain constant as the plunge pool erodes and the headcut retreats (see Figure 4). This formulation assumes that as the headcut retreats, the shape of the pool remains constant. Equation (2) is applied to existing gully headcuts, which are defined by the model as all locations where slopes (S) are steeper than 30% and where this slope

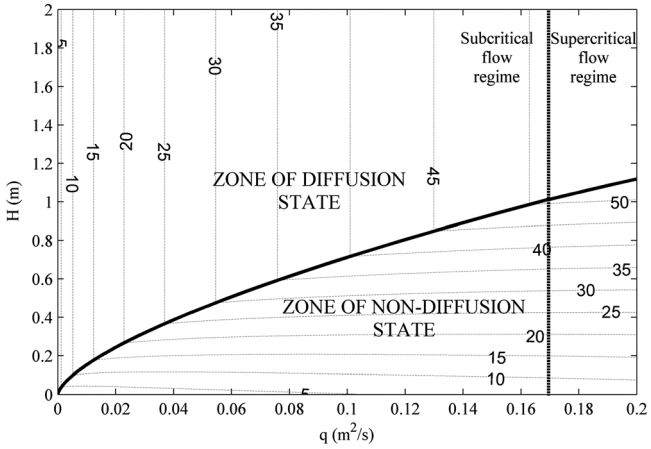

Figure 5. Shear stress at the bottom of the plunge pool as a function of discharge per unit width q and headcut height H (for $n = 0.04$, $S = 0.03$, and $S_f = 0.3$) in each of the four modes of plunge pool erosion: (a) diffusion and (b) nondiffusion states in a subcritical flow regime and (c) diffusion and (d) nondiffusion in a supercritical flow regime (based on *Flores-Cervantes et al*., [2006]).

is at least twice the downstream channel slope. The retreat rate is calculated for each precipitation pulse and stored. When the cumulative value is higher than the grid resolution, the upper node is eroded. The new channel slope at the bottom of the headcut is assumed to be equal to the previous downstream channel slope.

[20] The deepening rate is estimated as a function of the shear stress exceeding a certain threshold at the plunge pool bottom by water falling from the top of the headcut:

$$\frac{dD}{dt} = k(\tau - \tau_{cr})^p \tag{3}$$

where τ is the maximum shear stress produced at the bottom of the pool, τ_{cr} is the critical shear stress required for the scouring of the soil, and p is an empirical exponent, commonly 1 for cohesive soils [*Stein et al*., 1993; *Stein and Julien*, 1994; *Alonso et al*., 2002].

[21] The shear stress at the bottom of the pool can be calculated following the approach of *Alonso et al*. [2002]:

$$\tau = C_f \rho V_{\text{bottom}}^2 \tag{4}$$

where C_f is a coefficient of friction, ρ is the water density, and V_{bottom} is the maximum velocity of the flow at the bottom of the plunge pool produced by the impinging jet or potential core (Figure 4). Following *Alonso et al*. [2002], a Blasius flow assumption (irrotational flow along a flat surface) can be used to obtain C_f:

$$C_f = 0.025\left(\frac{\upsilon}{q}\right)^{0.2} \tag{5}$$

where v is the kinematic viscosity of water ($m^2\,s^{-1}$). V_{bottom} can be calculated in terms of the flow velocity at the brink (V_{brink}, Manning's equation), the pool geometry, and headcut height [*Flores-Cervantes et al*., 2006]. V_{bottom} depends on two conditions: the type of upstream flow approaching the edge of the headcut, which can be a subcritical or supercritical flow based on flow velocity at the brink, and the amount of diffusion of the water jet centerline impinging the plunge pool before it reaches the bottom of the pool. The core of the water falling in the plunge pool may or may not reach the bottom of the pool. If it reaches the bottom of the pool, the eroding shear stress at the bottom of the pool is a function of q and H. Alternatively, if the core is dampened as the water moves through the pool before reaching the bottom, a situation called "diffusion state" occurs as described by *Flores-Cervantes et al*. [2006]. In diffusion state, the eroding shear stress is only a function of q. Figure 5 illustrates very different effects of q and H when the jet centerline diffuses and when it does not. In our study, with our topographic conditions and discharge range, we found both states with a predominance of diffusion state.

[22] Therefore, the retreat rate is related to the flow conditions at the brink, the headcut height, the pool's shape, and soil characteristics.

3.3. Rainfall Disaggregation

[23] In CHILD, rainfall is represented as a succession of constant intensity pulses. Therefore, for each rainfall event, storm duration and intensity have to be defined, as well as

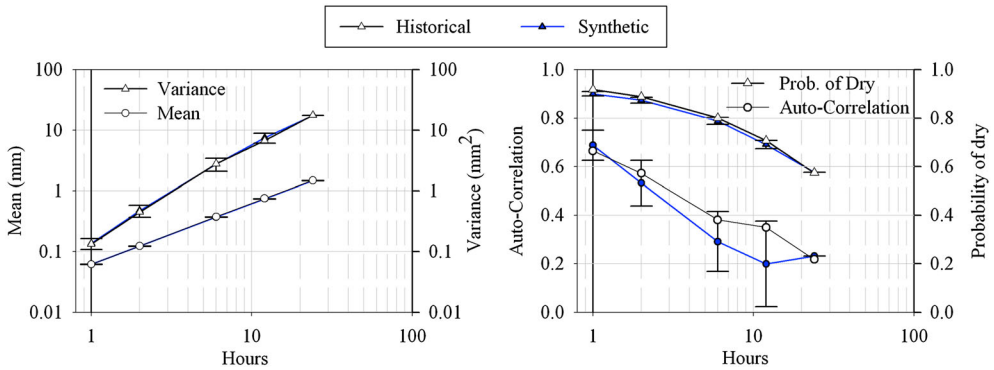

Figure 6. Historical and model statistics of cumulative precipitation: (left) mean rainfall depth and variance and (right) autocorrelation lag-1 and probability of dry periods, no rainfall. Values calculated from December months, from 1991 to 2009. Blue symbols represent model-disaggregated mean values, white historical. Error bars are twice the standard deviation of 10 disaggregation series.

Table 3. Estimated Parameters of MBL Model From Carcastillo Data Set

	Parameters					
Month	λ ($h^{-1} \times 10^3$)	κ	ϕ ($\times 10^{-1}$)	μ (mm h^{-1})	α	v (h)
January	9.91	0.28	0.99	1.14	9.14	8.41
February	8.65	5.93	1.21	0.12	10.43	7.78
March	7.72	7.00	1.13	0.16	13.21	7.18
April	9.47	3.19	4.66	0.38	6.56	13.54
May	8.87	0.21	0.63	1.80	12.69	11.49
Jun	7.30	0.25	0.66	3.25	40.00	20.00
July	4.34	2.17	7.92	1.06	7.99	12.31
August	4.76	4.69	5.02	0.98	7.08	4.62
September	6.02	0.85	2.91	1.10	3.93	6.93
October	8.46	0.27	1.26	1.61	7.13	9.27
November	8.55	0.13	0.82	1.51	5.22	8.17
December	9.54	0.11	0.38	2.15	28.61	19.49

time between pulses. To do this, daily rainfall data from the Carcastillo station from 1967 to 2003 (Figure 6) were disaggregated to hourly records. These hourly data were then used to run the CHILD simulations.

[24] Prior to executing the model runs using the disaggregated hourly rainfall, the disaggregation method was evaluated using subdaily (10 min) rainfall data available from 1991 onward. The term "rainfall disaggregation" indicates the generation of high-resolution rainfall time series adding up to prescribed longer-scale totals [*Marani and Zanetti*, 2007], which may be achieved by temporally partitioning the longer-scale amounts through a recursive rule [*Onof et al*., 2005] or by repeated adjustments of stochastic rainfall model runs [*Koutsoyiannis and Onof*, 2001]. Here the modified Bartlett-Lewis (MBL) stochastic rainfall model [*Rodríguez-Iturbe et al*., 1987], based on point processes theory [*Eagleson*, 1978], was used to disaggregate precipitation rainfall. The MBL model represents the arrival of rainfall events and of rain cells within events through a marked Poisson process. The arrival of storm events is described through a Poisson process with rate λ, in which the duration of storms is assumed to be exponentially distributed with rate γ. Within each storm, rain cells are generated through a second Poisson process with arrival rate β. Cells are characterized by exponentially distributed rainfall intensity (with parameter $1/\mu$) and duration (with parameter η). For mathematical convenience, two dimensionless parameters are introduced, $\kappa = \beta/\eta$ and $\phi = \gamma/\eta$. Here in order to incorporate the possibility of widely varying cell durations, the cell duration parameter η was set as a random variable that changes from storm to storm. The probability density function for η was assumed to be a two-parameter (shape parameter α and scale parameter v) gamma distribution. *Rodríguez-Iturbe et al*. [1988] found the analytical expressions of the first- and second-order moments of rainfall depth for different aggregation scales to be a function of six model parameters: λ, κ, ϕ, μ, α, and v. In this case, the MBL was calibrated using statistical characteristics of rainfall at 24 and 48 h. Moreover, the MBL was calibrated for each month, because patterns of rainfall are different for each month [*Rodríguez-Iturbe et al*., 1987]. The resulting parameters are shown in Table 3.

[25] Once the MBL was calibrated, the daily rainfall series was disaggregated into an hourly rainfall series. For each day or series of consecutive wet days, a series of synthetic hourly rainfall was generated with the MBL model until the measured daily rainfall was matched. For this, an algorithm that followed the methodology proposed by *Koutsoyiannis and Onof* [2001] was used. To account for the stochastic nature of the rainfall, 500 hourly rainfall series were generated that resulted in 500 simulation runs of CHILD.

[26] The disaggregation method was tested using high-resolution historical (1991–2009) precipitation series. The high-resolution data set was aggregated to the daily scale, MBL parameters were obtained from the aggregated data, and then the MBL parameters from the aggregated daily data were used to disaggregate back to an hourly rainfall series. Ten realizations of this aggregation/disaggregation were created and statistically compared. The main statistical properties (mean rainfall depth, variance, autocorrelation lag-1, and probability of dry periods (no rainfall)) were compared at several levels of aggregation from 1 to 24 h (Figure 6). Twice the standard deviation of 10 realizations was used to compute the 95% confidence interval for each statistic, assuming a normal distribution. Differences between disaggregated and measured rainfall series were minimal. These results are similar to those of *Koutsoyiannis and Onof* [2001], indicating a good performance of the disaggregation method in preserving the most important statistics of the rainfall events.

3.4. Model Calibration and Validation

[27] The gully model was calibrated using the initial boundary conditions of 1967 (DEM, 2 m pixel resolution) and the disaggregated rainfall series. The model was run for each of the 500 rainfall series using the same parameter set (Tables 1 and 4). Gully 1 was selected for calibration, as the contributing area and slope were representative of the area (Table 1). To calibrate the model, the linear headcut retreat and eroded soil volume were used as target variables, minimizing the difference between measured and simulated, and the form factor of the plunge pool S_f as the calibration parameter. The model depends on six parameters (S_f, c, n, p, τ_{cr}, and k) and on discharge and topography. Topography is a given input and discharge is model calculated from the rainfall. All six parameters, although physically defined, could be considered as calibration parameters and estimated using historical storm period, including several erosive storm events. Nevertheless, we considered c, n, p, τ_{cr}, and k as reasonably approximated from literature values (Table 4) and used S_f as the only calibration parameter. Headcut retreat is most sensitive to S_f, as reported by *Flores-Cervantes et al*. [2006] (see equation (2)). Furthermore, S_f is the only parameter specific to the headcut retreat module, meaning it does not affect any other process simulated in CHILD. Values of the shape factor reported in literature range between 0.02 and 0.64 [*Flores-Cervantes*, 2004]. In this study, the domain sampling of S_f was limited from 0.1 to 0.6, with increments of 0.01. We recognize that calibration in this manner is not

Table 4. Parameter Values Used in Model Simulation

Parameter	Value
Shape factor, S_f	0.31
Soil erodibility, k (m^3 $(N\,s)^{-1}$)	$2.54\ 10^{-8}$
Critical shear stress, τ_{cr} (Pa)	5
Erosion exponent, p	1
Manning's roughness, n	0.05
Grid size, c (m)	2

Table 5. Representative Values of the Erodibility and Critical Shear Stress Taken From the Literature

Shear Stress	Source	Soil Texture	k[a] (m^3 (N s)$^{-1}$)	τ_{cr} (Pa)
H[c]	*Knapen et al*. [2007]	Mean silt loam	2.3 10^{-5}	2.4
V[d]	*Hanson et al*. [2001]	Mean silt-bedded channels	3.5 10^{-7}	60
V[d]	*Potter et al*. [2002]	Mean silt loam	6.0 10^{-9}	-
H/V	*Knapen et al*. [2007]	Mean all data[b]	1.3 10^{-5}	7

[a]$\rho = 1400$ kg/m^3.
[b]From experiments (in laboratory flumes, field plots, and impinging submerged jet) reported in literature; 470 values of concentrated flow erodibility (k) and 522 of critical flow shear stress (τ_{cr}).
[c]Flow direction parallel to the soil surface.
[d]Flow direction perpendicular to the soil surface.

unique, since it is conditioned on other parameters that could potentially vary. Nevertheless, we feel this is the best approach because we can reasonably obtain values for other well-defined parameters from the literature and because calibration of other parameters, which affect other processes in the CHILD model, will increase the degrees of freedom and the uncertainty in the calibration process. That the calibrated S_f values (see following section) are within the ranges reported in the literature and measured at the site adds some confidence to the procedure.

[28] The selected Manning coefficient, n, of 0.05 corresponds to a floodplain with sparse brush and weeds [*Arcement and Schneider*, 1989]. The parameter p is set to 1 as discussed in the previous section. The values selected for k of 2.54 10^{-8} m^3 (N s)$^{-1}$ and τ_{cr} of 5 Pa produce little fluvial erosion during the period simulated, similar to what is observed in the field. The values selected for τ_{cr} and k fall within the ranges of values reported in literature (Table 5) [*Knapen et al*., 2007].

[29] In the set of simulations discussed here, the channel width c was assumed to be equal to 2 m. This assumption affected q, and thus, the headcut retreat rate. Measured headcut widths varied between 2 and 3.8 m. Thus, 2 m was representative of channel width in the simulations. Therefore, in the set of simulations, a DEM of 2 m resolution was used. The consequences of this assumption are further addressed in section 5.

[30] In order to validate the model, once the gully model was calibrated, the same parameter set was used to simulate the evolution of gullies 2–6.

4. Results

4.1. Measured Retreat Rates

[31] Measured linear and volumetric retreat rates of gully headcuts for different periods of time are shown in Table 2. Additionally, Figure 7 presents the evolution of the longitudinal profiles of each of gully, including the calibration gully (gully 1) and the gullies used for validation (gullies 2–6).

[32] During the first period (1967 to 1982), the mean linear measured headcut retreat rate was 0.57 m yr^{-1}; the maximum measured retreat rate was 1.80 m yr^{-1} and corresponded to the gully with the largest contributing area, gully 2 (8.51 ha). If gully 2 was not considered (this is what is shown in Table 2), the mean retreat rate was 0.32 m yr^{-1} and the maximum retreat 0.74 m yr^{-1} corresponding to gully 1. During the second time period (1982 to 2003), the mean and maximum linear headcut retreat rates were slightly higher, 0.41 m yr^{-1} and 0.78 m yr^{-1}, respectively. In this period, the maximum value was measured in gully 1.

[33] The above retreat rate estimates agree with previous studies in Bardenas by *Del Valle de Lersundi and Del Val* [1990], who report a retreat of 1.6 m over 2 years. Other studies, in relatively similar areas, show a retreat of 0.7 m yr^{-1} to 0.8 m yr^{-1} in Barasona (central Ebro Valley, Spain) and 0.2 m yr^{-1} in Penedes (eastern Pyrenees Basin, northeast Spain) [*Martínez-Casasnovas and Poch*, 1998; *Martínez-Casasnovas*, 2003].

[34] In terms of volumetric erosion, during the first period, the measured mean erosion rate was 3.88 m^3 yr^{-1}. The highest erosion rates occur at gully 2 (see Table 2). During the second period, volumetric erosion rates increased for each gully, except for gully 2. If gully 2 is not considered, the mean volumetric retreat rates, shown in Table 2, are 1.59 m^3 yr^{-1} and 2.20 m^3 yr^{-1}, for the first and second time periods, respectively.

[35] Erosion rate in terms of mass eroded per unit contributing area (estimated by multiplying the volumetric erosion rate by the average measured bulk density of the soils and dividing by the contributing area corresponding to each gully headcut) had a mean value of 0.40 kg m^{-2} yr^{-1} during the first period and 0.51 kg m^{-2} yr^{-1} in the second period. For the complete simulation (36 years), the mean erosion rate was 0.46 kg m^{-2} yr^{-1}. This value is similar to reported data (0.15-0.75 kg m^{-2} yr^{-1}) from *Vandekerckhove et al*. [2003] in southeast Spain for a 20–40 year time period.

4.2. Calibration

[36] Simulated and measured erosion rates (in terms of linear headcut retreat and volume) for gully 1 matched best with an S_f of 0.31. This calibrated value is similar to the mean measured S_f (0.35) in the study area. Measured retreat at gully 1 was 27.1 ± 0.3 m, corresponding to an eroded soil volume of 65.0 ± 8 m^3 over the 36 year period. For all 500 realizations, each one with a different hourly rainfall series and all using the same calibration parameter set, the mean retreat estimated with the calibrated S_f was 26.4 ± 0.2 m and an associated mean eroded soil volume of 65.1 ± 0.5 m^3 (Table 2).

[37] The measured and simulated longitudinal profiles of the evolution of gully 1 are shown in Figure 7. Twice the standard deviation of the retreat rate of the 500 model realizations was used to compute the 95% confidence interval (CI) of retreat shown in the figure. For every gully headcut simulated, retreats are in a narrow range. In gully 1, the CI is lower than 0.4 m for the whole 36 years, so the filled area in Figure 7 is behind and partly covered by the mean simulated longitudinal profile. As can be seen, the original profile of the headcut in the 1967 measurement data was more vertical than that simulated at time zero. This is because simulated profiles were plotted by linking Voronoi nodes that are separated by 2 m, instead of plotting the surfaces of Voronoi cells. Taking as a reference point the top bank of the headcut, it is observed that the retreat rates measured in all 500 realizations simulated after the calibration of gully 1 for the 36 year study differ by only 3%.

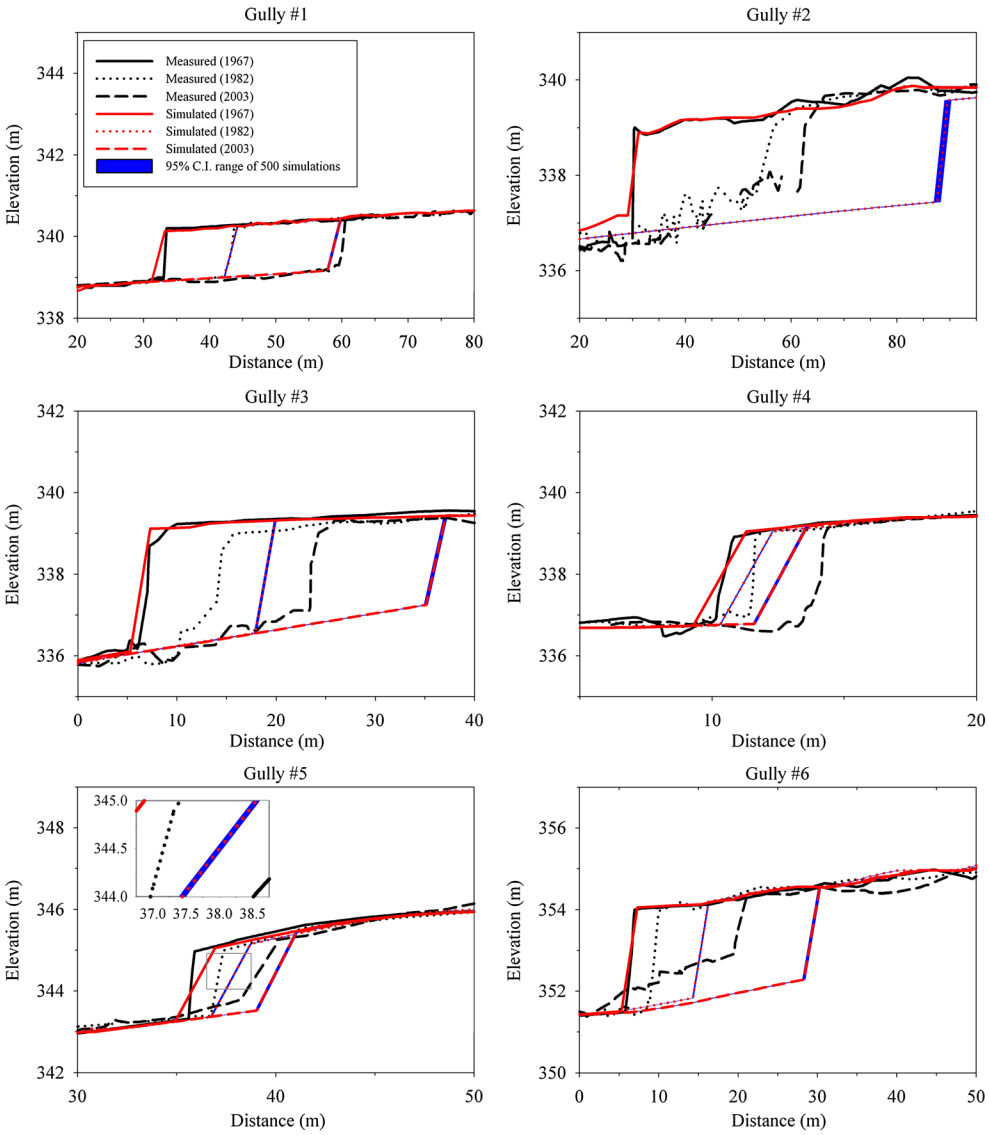

Figure 7. Evolution of the measured and simulated longitudinal profiles of each of the studied gullies. The location of headcuts is shown in each time step where measured data were available: 1967, 1982, and 2003. Mean simulated retreat of the 500 model realizations is presented in red. The 95% confidence interval range of simulations is represented in blue filled area (detail zoom in gully 5). Gully 1 is used for calibration while the remaining ones are used for validation.

[38] The mean eroded volume resulting from gully 1, the calibration gully, in the 36 year simulation was exactly estimated by the model (Table 2).

4.3. Validation

[39] The parameters determined above were used to simulate the evolution of gullies 2–6. The results are provided in Table 2 and Figures 7 and 8. For the 36 year simulation period, the model overestimated the measured linear retreat on validation gullies by 54% (Table 2). Maximum overestimation values were observed on the widest gullies in this study, with overestimation of 76% for gully 6 (3.8 m width) and 67% for gully 3 (3.5 m width) (Figure 7).

[40] During the first period, similar results were found, with a linear relationship between simulated and measured linear retreat of $r^2 = 0.98$ (Figure 8a). Again, headcut retreat overestimation was larger and proportional on the widest gullies (Tables 1 and 2). However, gullies having a width close to the channel width used in the simulations (2 m) had errors lower than 20%. This is the case of gullies 5 and 4, with a real width of 2.4 m and 2.6 m, respectively. Measured retreat for gullies 5 and 4 was 1.5 ± 0.3 m and 1.1 ± 0.3 m, respectively, from 1967 to 1982, whereas CHILD simulated a mean retreat of 1.8 ± 0.05 m and 1.0 ± 0.03 m for the 500 simulations (Table 2).

[41] Figure 8b shows the measured versus simulated eroded soil volume resulting from the headcut retreat, including the calibration headcut. As described in section 3.1, at some unknown date, the drainage pattern in gully 2 changed, and hence, we decided to remove it from the second period analyzed in this study. During the 36 year period analyzed, there was a good linear relationship between the total eroded soil

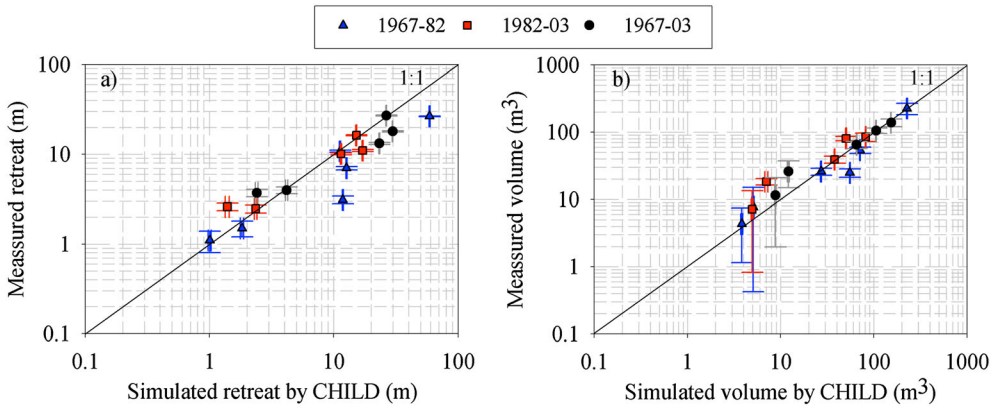

Figure 8. Measured versus simulated linear and volumetric retreat. Measured errors and 95% confidence interval of simulations are represented by error bars.

volume derived from the DEMs and those simulated by the model: $r^2 = 0.98$, with a 5% overestimation by the model. It is remarkable that for the whole period and for the four validation gullies, the 95% confidence interval of simulated volumetric retreat is less than 1 m^3.

[42] In the first period, based on a linear relationship, the model overestimated the measured volume of eroded soil by 3% (Figure 8b) in all five validation gullies ($r^2 = 0.96$). During the next period, 1982–2003, the model underestimated the measured volume of soil eroded by 21%, excluding gully 2 ($r^2 = 0.89$).

5. Discussion

[43] For the 36 year simulation, 1967–2003, CHILD predicts the volume rates of eroded soil properly. The annual average volume of soil eroded was really close between simulations and observations with a value of 1.93 m^3 yr^{-1}, and 1.95 m^3 yr^{-1}, respectively. Conversely, CHILD overestimated gully headcut retreat. The annual average retreat measured for the whole period is 0.37 m yr^{-1}, whereas simulations predict 0.48 m yr^{-1}. This discrepancy becomes larger when comparing the average retreat in gully 2 for the first period, where the simulated retreat rate is 4.01 ± 0.04 m yr^{-1}, against the measured 1.80 ± 0.02 m yr^{-1}. The simulated linear retreat is a biased estimate of erosion and does not account for the gully cross-section variability (width and depth). In the simulations, the channel width was fixed at 2 m, both in model calibration and validation, which has some implications from the modeling perspective. Fitting a constant channel width affects the unit discharge q, and hence the shear stress at the pool bottom τ. A narrower channel width results in a larger unit discharge and, consequently, in a faster headcut retreat.

[44] In order to ascertain the channel width influence in the linear and volumetric gully headcut retreat, we recalculated the retreat for different channel widths by varying the grid resolution in CHILD. Due to the close similarity among the 500 realizations in the previous modeling exercise, we have used just one realization for each gully and channel width in this analysis. As an example, Figure 9 shows the linear and volumetric retreats over the 36 year studied period for gully 3 using different channel widths; channel width was set per DEM resolution. For the 36 year period analyzed, headcut retreat increases by 120% on average, when channel width decreases from 2 m to 1 m. Nevertheless, volumetric

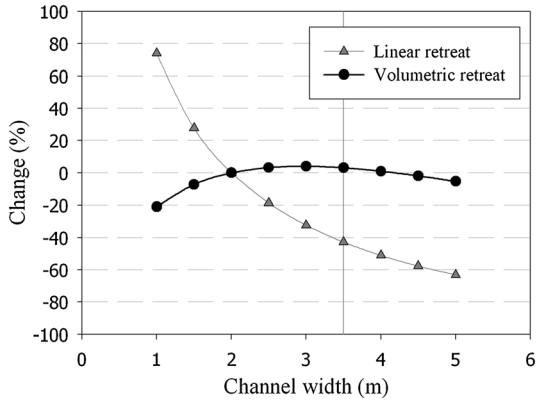

Figure 9. Effect of channel width variation on simulated linear retreat and volumetric retreat on gully 3.

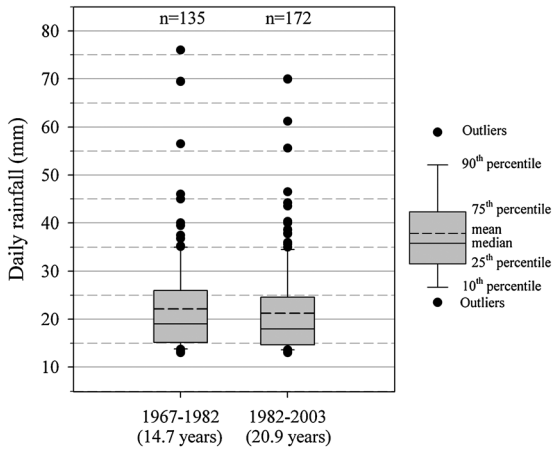

Figure 10. Distribution of daily precipitation higher than 10 mm d^{-1} for both periods analyzed, first 1967–1982 (14.7 years) and second 1982–2003 (20.9 years).

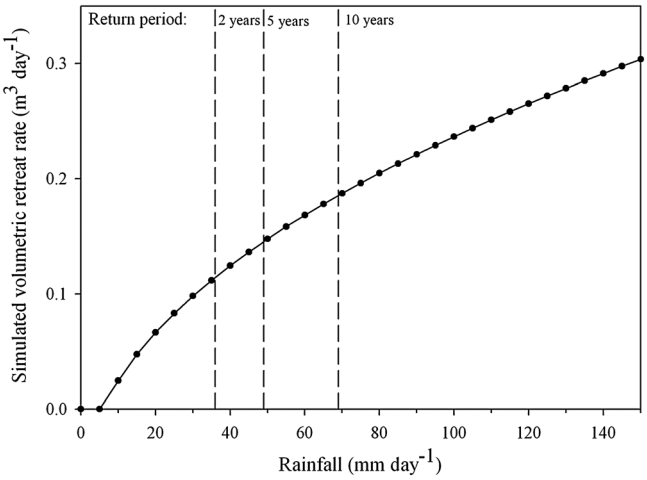

Figure 11. Influence of rainfall intensity on simulated volumetric retreat. Simulations carried out on gully 1 with daily constant pulse of rainfall.

erosion changes are less than 25%. Since volumetric erosion is the product of channel width per headcut retreat and height, the increase in the retreat compensates the decrease in channel width. Conversely, if channel width is set to 3.5 m, the modeled retreat rates improve, with a reduction in retreat rate of 43%, 36%, and 27% for gullies 3, 6, and 2, respectively. Volumetric erosion increases little, less than 10% in gullies 3 and 6. For the whole period of study and considering five gullies, the coefficient of determination of linear retreat increases from 0.76 to 0.98. Thus, the linear headcut retreat is more sensitive to channel width than the volumetric retreat. In addition, the volumetric retreat remains similar for different channel widths (Figure 9).

[45] Concerning the temporal evolution of the study gullies, the measured erosion rates were higher in the second period analyzed, 1982–2003, than the first one, 1967–1982 (see Table 2). This fact can be due to a different pattern of rainfall in both periods. Thus, adopting *Wischmeier and Smith*'s [1978] the rain erosivity threshold of 13 mm per day, we can explore the role of rainfall on gully headcut retreat. In our study area, the average number of days with rainfall higher than 13 mm was slightly lower in the second period (8.2 day yr^{-1}) than in the first one (9.3 day yr^{-1}) (Figure 10). The average daily precipitation for days with rainfall greater than 13 mm for the first and second periods was 22.1 mm d^{-1} and 21.2 mm d^{-1}, respectively. Nevertheless, if we focus our attention on heavy storms, i.e., daily precipitation higher than 30 mm d^{-1}, then the first period had 21 events versus 26 events in the second period. This difference in the occurrence of heavy storm events was one of the main gully erosion drivers. However, this relationship has been poorly studied. One of the few studies on this relationship was carried out by *Capra et al*. [2009] in Sicily (Italy), highlighting that gully erosion is directly and mainly controlled by rainfall events. *Capra et al*. [2009] found that the eroded volume was related to the maximum value of 3 day rainfall and by the maximum intensity of 1 h rainfall (power-type equation). Therefore, gully headcut retreat is a nonlinear process dominated by extreme events, which is in agreement with compiled references by *Poesen et al*. [2002] and also indicated by *Martínez-Casasnovas et al*. [2004].

[46] Despite higher measured erosion rates in the second period, CHILD simulated a slightly higher volumetric activity in the first period for five out of the six gullies. A possible explanation for this behavior is the linear behavior of CHILD during intense rainfall events, underestimating the actual, observed response. To explore this idea, we simulated the volumetric headcut retreat on gully 1 under different synthetic rainfall pulses of constant intensity during 24 h (Figure 11). For daily rainfall events with return period higher than 2 years (lower frequency), the relationship between simulated volumetric retreat rate and rainfall intensity became linear, in contrast to the results in *Capra et al*. [2009]. The model response to rainfall intensity (Figure 11) follows the same pattern as shear stress response to unit discharge in the diffusive state (Figure 5), which is the predominant state in our study. This is the case for gully 1, 1.2 m height, used for simulations shown in Figure 11. This similar behavior can be explained due to the relationship between headcut retreat rate and the shear stress at the bottom of the pool being linear, once a critical shear stress is overpassed (equations (2) and (3)). Therefore, the relationship between headcut retreat and rainfall intensity follows the same pattern as τ and q (Figure 5). An increase of rainfall intensity at lower values (and then unit discharge) produces a nonlinear increase on shear stress at the bottom of the pool (Figure 5). However, with an increase at extreme rainfall intensities, this behavior becomes linear. Consequently, extreme erosive storms, with high hourly rainfall intensity, could be underestimated by CHILD and small erosive storms overestimated. The same pattern has been found with AnnAGNPS model [*Taguas et al*., 2012]. This explains how the erosion model follows the trend of average precipitation more in the first period than on the second one.

[47] It is noteworthy that the headcut retreat module in CHILD was calibrated with all soil parameters constant throughout the 36 year simulation. Actually, this is a simplification of reality. Soil erodibility and critical shear stress are functions of many variables [e.g., *Foster* 1986; *Cerdà and Doerr*, 2007], among them soil moisture and land cover. Modeling soil resistance as a function of land cover is one of the main goals of future work [*Tucker and Hancock*, 2010]. Land cover appears to be a dominant variable in gully stabilization and therefore necessary to consider in the process of soil erosion [*Martínez-Casasnovas et al*., 2009; *Marzolff et al*., 2011].

[48] As a final point, to deal with channel width limitation, the gully width in future versions of the model should be considered variable. It could possibly be determined using an empirical relationship, such as a function of flow discharge or the contributing area [*Nachtergaele et al*., 2002; *Torri et al*., 2006; *Wells et al*., 2013].

6. Conclusions

[49] In this paper, we presented the results of a 36 year study of six gully headcuts due to plunge pool using a combination of multitemporal aerial photographs for gully measurements in a watershed within the Ebro Valley (Spain), and simulations using the CHILD model with a gully headcut retreat module. The model was calibrated with the shape factor S_f. The calibrated S_f was in agreement with field measurements in the region of Bardenas. Volumes of eroded soil were well predicted by CHILD. However, retreat was overestimated during

the validation, apparently due to the assumption of fixed gully width.

[50] In CHILD, as in the majority of landscape evolution models, one of the main limitations is the assumption that cells have fixed size (gully width) and erosion is applied over a whole (single) cell. This study shows that the gully width is an essential factor to improve the quality of the simulation matching measured and simulated retreats. In spite of the channel width limitation, the model's estimates of eroded soil volume match the observations well and these estimates were not very sensitive to channel width. This property is very useful, for example, in estimating soil erosion due to gully headcut retreat erosion in a watershed that terminates in a lake or reservoir. Furthermore, the gully headcut module in CHILD is capable of exploring other processes, such as bank failure and sedimentation, which were not analyzed in this work. All of which permits the investigation of the interaction and competition between these processes.

[51] The results of rainfall disaggregation showed a good performance of the methodology in preserving the most important statistical properties of the rainfall process. Thus, in future efforts, this methodology could be useful for downscaling general circulation models to finer time scales [*Onof and Arnbjerg-Nielsen*, 2009] and predicting gully evolution under different climate scenarios.

[52] This study has provided a first evaluation of the gully headcut retreat due to plunge pool erosion module, implemented in CHILD [*Flores-Cervantes et al.*, 2006].

[53] **Acknowledgments.** This work was made possible by financial support from the Spanish Ministry of Science and Technology, through the research project CGL2007-63453/HID, the Department of Education of the Government of Navarra, and the Public University of Navarra, with a fellowship awarded to the first author. The authors acknowledge the assistance of Tracasa Company and the Natural Park Administration "Junta de Bardenas." The authors also acknowledge the computing facilities of the Department of Civil and Environmental Engineering at the Massachusetts Institute of Technology. CHILD development was supported by the U.S. Army Research Office (agreement DAAD 19-01-1-0513) and through the NSF grant (EAR 0642550).

References

Alonso, C. V., S. J. Bennett, and O. R. Stein (2002), Predicting head cut erosion and migration in concentrated flows typical of upland areas, *Water Resour. Res.*, *38*(12), 1303, doi:10.1029/2001WR001173.

Arcement, G. J., and V. R. Schneider (1989), Guide for selecting Manning's roughness coefficients for natural channels and flood plains, *U.S. Geol. Surv. Water-Supply Pap.*, *2339*, 1–38.

Bennett, S. J. (1999), Effect of slope on the growth and migration of headcuts in rills, *Geomorphology*, 30(3), 273–290, doi:10.1016/S0169-555X(99)00035-5.

Bennett, S. J., and C. V. Alonso (2005), Modeling headcut development and migration in upland concentrated flows, *Int. J. Sedimemt. Res.*, *20*(4), 281–294.

Bennett, S. J., and J. Casalí (2001), Effect of initial step height on headcut development in upland concentrated flows, *Water Resour. Res.*, *37*(5), 1475–1484, doi:10.1029/2000WR900373.

Bennett, S. J., C. V. Alonso, S. N. Prasad, and M. J. M. Römkens (2000), Experiments on headcut growth and migration in concentrated flows typical of upland areas, *Water Resour. Res.*, *36*(7), 1911–1922, doi:10.1029/2000WR900067.

Bingner, R. L., F. D. Theurer, and Y. Yuan (2009), Agricultural non-point source pollution model. AnnAGNPS Technical Processes Documentation Version 5.0., USDA-ARS-NRCS, Oxford (MS).

Bradford, J. M., and R. P. Piest (1980), Erosional development of valley-bottom gullies in the upper Midwestern United States, in *Thresholds in Geomorphology*, edited by D. Coates and J. D. Vitek, pp. 75–101, Allen and Unwin, Londres.

Braun, J., and M. Sambridge (1997), Modelling landscape evolution on geological time scales: A new method based on irregular spatial discretization, *Basin Res.*, *9*(1), 27–52, doi:10.1046/j.1365-2117.1997.00030.x.

Campo, M. A., J. Álvarez-Mozos, J. Casalí, L. M. De Santisteban, R. Giménez, and J. A. Martínez-Casasnovas (2006), Long term evolution assessment of the permanent gully network in Las Bardenas Reales area (Navarre, Spain) influenced by land use change, paper presented at *Soil and Water Conservation Under Changing Land Use*, Lleida Univ. Press., Lleida, Spain.

Capra, A., P. Porto, and B. Scicolone (2009), Relationships between rainfall characteristics and ephemeral gully erosion in a cultivated catchment in Sicily (Italy), *Soil Tillage Res.*, *105*(1), 77–87, doi:10.1016/j.still.2009.05.009.

Casalí, J., J. J. Lopez, and J. V. Giraldez (1999), Ephemeral gully erosion in southern Navarra (Spain), *Catena*, *36*(1-2), 65–84, doi:10.1016/S0341-8162(99)00013-2.

Cerdà, A., and S. H. Doerr (2007), Soil wettability, runoff and erodibility of major dry-Mediterranean land use types on calcareous soils, *Hydrol. Processes*, *21*(17), 2325–2336, doi:10.1002/hyp.6755.

Coulthard, T. J. (2001), Landscape evolution models: A software review, *Hydrol. Processes*, *15*(1), 165–173, doi:10.1002/hyp.426.

Daba, S., W. Rieger, and P. Strauss (2003), Assessment of gully erosion in eastern Ethiopia using photogrammetric techniques, *Catena*, *50*(2-4), 273–291, doi:10.1016/S0341-8162(02)00135-2.

Day, P. R. (1965), Particle fractionation and particle-size analysis, in *Methods of Soil Analysis, Part 1*, edited by C. A. Black, pp. 545–567, American Society of Agronomy, Madison, Wisconsin, USA.

De Ploey, J. (1989), A model for headcut retreat in rills and gullies, *Catena Suppl.*, *14*, 81–86.

De Ploey, J. (1990), Threshold conditions for thalweg gullying with special reference to loess areas, *Catena Suppl.*, *17*, 147–151.

De Santisteban, L. M., J. Casalí, and J. J. López (2005), Evaluation of rill and ephemeral gully erosion in cultivated areas of Navarre (Spain), *Int. J. Sediment. Res.*, *20*(3), 270–280.

De Santisteban, L. M., J. Casalí, and J. J. Lopez (2006), Assessing soil erosion rates in cultivated areas of Navarre (Spain), *Earth Surf. Processes Landforms*, *31*(4), 487–506, doi:10.1002/esp.1281.

Del Valle De Lersundi, J. M., and J. Del Val (1990), Procesos de erosión y análisis de sus condicionantes en una región semi-árida: La Cuenca de Cornialto (Bardenas, Navarra), *Cuat y Geomorfología*, *4*, 55–67.

Derose, R. C., B. Gomez, M. Marden, and N. A. Trustrum (1998), Gully erosion in Mangatu forest, New Zealand, estimated from digital elevation models, *Earth Surf. Processes Landforms*, *23*(11), 1045–1053, doi:10.1002/(SICI)1096-9837(1998110)23:11<1045::AID-ESP920>3.0.CO;2-T.

Dey, A. K., T. Tsujimoto, and T. Kitamura (2001), Growth and migration of headcut in heterogeneous soil stratum, *Ann. J. Hydraul. Eng. JASCE*, *45*, 823–828.

Eagleson, P. S. (1978), Climate, soil, and vegetation: 2. The distribution of annual precipitation derived from observed storm sequences, *Water Resour. Res.*, *14*(5), 713–721.

Flores-Cervantes, J. H. (2004), Headcut retreat resulting from plunge pool erosion in a 3D landscape evolution model, MS thesis, Massachusetts Institute of Technology, Cambridge, MA, USA.

Flores-Cervantes, J. H., E. Istanbulluoglu, and R. L. Bras (2006), Development of gullies on the landscape: A model of headcut retreat resulting from plunge pool erosion, *J. Geophys. Res.*, *111*, F01010, doi:10.1029/2004JF000226.

Foster, G. R. (1986), Understanding ephemeral gully erosion, in *Soil Conservation: An Assessment of the National Resources Inventory*, vol. 2, edited by Anonymous, pp. 90–128, National Academy Press, Washington, D. C.

Gimenez, R., I. Marzolff, M. A. Campo, M. Seeger, J. B. Ries, J. Casalí, and J. Álvarez-Mozos (2009), Accuracy of high-resolution photogrammetric measurements of gullies with contrasting morphology, *Earth Surf. Processes Landforms*, *34*(14), 1915–1926, doi:10.1002/esp.1868.

Gordon, L. M., S. J. Bennett, R. L. Bingner, F. D. Theurer, and C. V. Alonso (2007), Simulating ephemeral gully erosion in AnnAGNPS, *Trans. ASABE*, *50*(3), 857–866.

Gordon, L. M., S. J. Bennett, C. V. Alonso, and R. L. Bingner (2008), Modeling long-term soil losses on agricultural fields due to ephemeral gully erosion, *J. Soil Water Conserv.*, *63*(4), 173–181, doi:10.2489/jswc.63.4.173.

Grossman, R. B., and T. G. Reinsch (2002), 2.1 Bulk density and linear extensibility, in *Methods of Soil Analysis: Part 4 Physical Methods*, SSSA Book Series, edited by J. H. Dane and G. C. Topp, pp. 201–228, Soil Science Society of America, Madison, WI, USA.

Hanson, G. J., K. M. Robinson, and K. R. Cook (2001), Prediction of headcut migration using a deterministic approach, *Trans. ASAE*, *44*(3), 525–531.

Hapke, C. J. (2005), Estimation of regional material yield from coastal landslides based on historical digital terrain modelling, *Earth Surf. Processes Landforms*, *30*(6), 679–697, doi:10.1002/esp.1168.

Heede, B. H. (1976), *Gully Development and Control: The Status of our Knowledge*, Rocky Mountain Forest and Range Experiment Station, Forest Service, U.S. Dept. of Agriculture, Fort Collins, CO.

Hengl, T. (2006), Finding the right pixel size, *Comput. Geosci.*, *32*(9), 1283–1298, doi:10.1016/j.cageo.2005.11.008.

Howard, A. D. (1994), A detachment-limited model of drainage-basin evolution, *Water Resour. Res.*, *30*(7), 2261–2285, doi:10.1029/94WR00757.

Howard, A. D., and C. F. McLane (1988), Erosion of cohesionless sediment by groundwater seepage, *Water Resour. Res.*, *24*(10), 1659–1674.

Ireland, H. A., D. H. Eargle, and C. F. S. Sharpe (1939), *Principles of Gully Erosion in the Piedmont of South Carolina*, Division of Research, Soil Conservation Services, U.S. Government Printing Office, Washington, D. C.

Istanbulluoglu, E., R. L. Bras, H. Flores-Cervantes, and G. E. Tucker (2005), Implications of bank failures and fluvial erosion for gully development: Field observations and modeling, *J. Geophys. Res.*, *110*, F01014, doi:10.1029/2004JF000145.

Knapen, A., J. Poesen, G. Govers, G. Gyssels, and J. Nachtergaele (2007), Resistance of soils to concentrated flow erosion: A review, *Earth Sci. Rev.*, *80*(1-2), 75–109, doi:10.1016/j.earscirev.2006.08.001.

Koutsoyiannis, D., and C. Onof (2001), Rainfall disaggregation using adjusting procedures on a Poisson cluster model, *J. Hydrol.*, *246*(1-4), 109–122, doi:10.1016/S0022-1694(01)00363-8.

Larrasoaña, J. C., X. Murelaga, and M. Garcés (2006), Magnetobiochronology of Lower Miocene (Ramblian) continental sediments from the Tudela Formation (western Ebro basin, Spain), *Earth Planet. Sci. Lett.*, *243*(3-4), 409–423, doi:10.1016/j.epsl.2006.01.034.

Leopold, L. B., M. G. Wolman, and J. P. Miller (1964), *Fluvial Processes in Geomorphology*, Courier Dover Publications, New York.

Lobkovsky, A. E., B. E. Smith, A. Kudrolli, D. C. Mohrig, and D. H. Rothman (2007), Erosive dynamics of channels incised by subsurface water flow, *J. Geophys. Res.*, *112*, F03S12, doi:10.1029/2006JF000517.

Marani, M., and S. Zanetti (2007), Downscaling rainfall temporal variability, *Water Resour. Res.*, *43*, W09415, doi:10.1029/2006WR005505.

Martínez-Casasnovas, J. A. (2003), A spatial information technology approach for the mapping and quantification of gully erosion, *Catena*, *50*(2-4), 293–308, doi:10.1016/S0341-8162(02)00134-0.

Martínez-Casasnovas, J. A., and R. M. Poch (1998), Estado de conservación de los suelos de la cuenca del embalse Joaquín Costa, *Limnetica*, *14*, 83–91.

Martínez-Casasnovas, J. A., C. Antón-Fernández, and M. C. Ramos (2003), Sediment production in large gullies of the Mediterranean area (NE Spain) from high-resolution digital elevation models and geographical information systems analysis, *Earth Surf. Processes Landforms*, *28*(5), 443–456, doi:10.1002/esp.451.

Martínez-Casasnovas, J. A., M. C. Ramos, and J. Poesen (2004), Assessment of sidewall erosion in large gullies using multi-temporal DEMs and logistic regression analysis, *Geomorphology*, *58*(1-4), 305–321.

Martínez-Casasnovas, J. A., M. Concepcion Ramos, and D. Garcia-Hernandez (2009), Effects of land-use changes in vegetation cover and sidewall erosion in a gully head of the Penedes region (northeast Spain), *Earth Surf. Processes Landforms*, *34*(14), 1927–1937, doi:10.1002/esp.1870.

Marzolff, I., J. B. Ries, and J. Poesen (2011), Short-term versus medium-term monitoring for detecting gully-erosion variability in a Mediterranean environment, *Earth Surf. Processes Landforms*, *36*(12), 1604–1623, doi:10.1002/esp.2172.

Momm, H. G., R. L. Bingner, R. R. Wells, and D. Wilcox (2012), AGNPS GIS-based tool for watershed-scale identification and mapping of cropland potential ephemeral gullies, *Appl. Eng. Agric.*, *28*(1), 17–29.

Moore, J. S., D. M. Temple, and H. A. D. Kirsten (1994), Headcut advance threshold in earth spillways, *Bull. Geol. Soc. Am.*, *31*, 277–280.

Nachtergaele, J., and J. Poesen (1999), Assessment of soil losses by ephemeral gully erosion using high-altitude (stereo) aerial photographs, *Earth Surf. Processes Landforms*, *24*(8), 693–706.

Nachtergaele, J., J. Poesen, A. Sidorchuk, and D. Torri (2002), Prediction of concentrated flow width in ephemeral gully channels, *Hydrol. Proc.*, *16*(10), 1935–1953, doi:10.1002/hyp.392.

Nazari Samani, A., H. Ahmadi, A. Mohammadi, J. Ghoddousi, A. Salajegheh, G. Boggs, and R. Pishyar (2010), Factors controlling gully advancement and models evaluation (Hableh Rood Basin, Iran), *Water Resour. Manage.*, *24*(8), 1531–1549, doi:10.1007/s11269-009-9512-4.

Onof, C., and K. Arnbjerg-Nielsen (2009), Quantification of anticipated future changes in high resolution design rainfall for urban areas, *Atmos. Res.*, *92*(3), 350–363, doi:10.1016/j.atmosres.2009.01.014.

Onof, C., J. Townend, and R. Kee (2005), Comparison of two hourly to 5-min rainfall disaggregators, *Atmos. Res.*, *77*(1-4 SPEC. ISS.), 176–187, doi:10.1016/j.atmosres.2004.10.022.

Oostwoud Wijdenes, D. J., and R. B. Bryan (1994), Gully headcuts as sediment sources on the Njemps flats and initial low-cost gully control measures, *Catena Suppl.*, *27*, 205–229.

Oostwoud Wijdenes, D. J., J. Poesen, L. Vandekerckhove, and M. Ghesquiere (2000), Spatial distribution of gully head activity and sediment supply along an ephemeral channel in a Mediterranean environment, *Catena*, *39*(3), 147–167, doi:10.1016/S0341-8162(99)00092-2.

Poesen, J., L. Vandekerckhove, J. Nachtergaele, D. Oostwoud Wijdenes, G. Verstraeten, and B. Van Wesemael (2002), Gully erosion in dryland environments, in *Dryland Rivers: Hydrology and Geomorphology of Semi-Arid Channels*, edited by L. J. Bull and M. J. Kirkby, pp. 229–262, Wiley, Chichester, UK.

Poesen, J., J. Nachtergaele, G. Verstraeten, and C. Valentin (2003), Gully erosion and environmental change: Importance and research needs, *Catena*, *50*(2-4), 91–133, doi:10.1016/S0341-8162(02)00143-1.

Potter, K. N., J. D. J. Velázquez-Garcia, and H. A. Torbert (2002), Use of a submerged jet device to determine channel erodibility coefficients of selected soils of Mexico, *J. Soil Water Conserv.*, *57*(5), 272–277.

Powledge, G. R., D. C. Ralston, P. Miller, H. C. Yung, P. E. Clopper, and D. M. Temple (1989), Mechanics of overflow erosion on embankments. I. Research activities, *J. Hydraul. Eng. ASCE*, *115*(8), 1040–1055.

Rieke-Zapp, D. H., and M. H. Nichols (2011), Headcut retreat in a semiarid watershed in the southwestern United States since 1935, *Catena*, *87*(1), 1–10, doi:10.1016/j.catena.2011.04.002.

Ries, J. B., and I. Marzolff (2003), Monitoring of gully erosion in the central Ebro Basin by large-scale aerial photography taken from a remotely controlled blimp, *Catena*, *50*(2-4), 309–328, doi:10.1016/S0341-8162(02)00133-9.

Robinson, K. M. (1989), Hydraulic stresses on an overfall boundary, *Trans. ASAE*, *32*(4), 1269–1274.

Rodríguez-Iturbe, I., D. R. Cox, and V. Isham (1987), Some models for rainfall based on stochastic point processes, *Proc. R. Soc. London, Ser. A*, *410*(1839), 269–288.

Rodríguez-Iturbe, I., D. R. Cox, and V. Isham (1988), A point process model for rainfall: Further developments, *Proc. R. Soc. London, Ser. A*, *417*(1853), 283–298.

Sancho, C., J. L. Peña, A. Muñoz, G. Benito, E. McDonald, E. J. Rhodes, and L. A. Longares (2008), Holocene alluvial morphopedosedimentary record and environmental changes in the Bardenas Reales Natural Park (NE Spain), *Catena*, *73*(3), 225–238, doi:10.1016/j.catena.2007.09.011.

Seeger, M., I. Marzolff, and J. B. Ries (2009), Identification of gully-development processes in semi-arid NE-Spain Zeit, *Geomorphology*, *53*(4), 417–431.

Seginer, I. (1966), Gully development and sediment yield, *J. Hydrol.*, *4*, 236–253.

Sidorchuk, A. (1999), Dynamic and static models of gully erosion, *Catena*, *37*(3-4), 401–414, doi:10.1016/S0341-8162(99)00029-6.

Smith, L. (1992), *Investigation of Ephemeral Gullies in Loessial Soils in Mississippi*, U.S. Army Corps of Engineers Waterways Experiment Station, Vicksburg, MS, USA.

SSSA (2001), *Glossary of Soil Science Terms*, SSSA, Madison, WI.

Stein, O. R., and P. Y. Julien (1993), Criterion delineating the mode of headcut migration, *J. Hydraul. Eng. ASCE*, *119*(1), 37–50.

Stein, O. R., and P. Y. Julien (1994), Sediment concentration below free overfall, *J. Hydraul. Eng. ASCE*, *120*(9), 1043–1059.

Stein, O. R., C. V. Alonso, and P. Y. Julien (1993), Mechanics of jet scour downstream of a headcut, *J. Hydraul. Eng. ASCE*, *31*(6), 723–738.

Taguas, E. V., Y. Yuan, R. L. Bingner, and J. A. Gomez (2012), Modeling the contribution of ephemeral gully erosion under different soil managements: A case study in an olive orchard microcatchment using the AnnAGNPS model, *Catena*, *98*, 1–16, doi:10.1016/j.catena.2012.06.002.

Tebebu, T. Y., et al. (2010), Surface and subsurface flow effect on permanent gully formation and upland erosion near Lake Tana in the northern highlands of Ethiopia, *Hydrol. Earth Syst. Sci.*, *14*(11), 2207–2217, doi:10.5194/hess-14-2207-2010.

Temple, D. M., and G. J. Hanson (1994), Headcut development in vegetated earth spillways, *Appl. Eng. Agric.*, *10*(5), 677–682.

Thompson, J. R. (1964), Quantitative effect of watershed variables on rate of gully-head advancement, *Trans. ASAE*, *7*(1), 54–55.

Torri, D., J. Poesen, L. Borselli, and A. Knapen (2006), Channel width-flow discharge relationships for rills and gullies, *Geomorphology*, *76*(3-4), 273–279, doi:10.1016/j.geomorph.2005.11.010.

Tucker, G. E., and G. R. Hancock (2010), Modelling landscape evolution, *Earth Surf. Processes Landforms*, *35*(1), 28–50, doi:10.1002/esp.1952.

Tucker, G. E., S. T. Lancaster, N. M. Gasparini, and R. L. Bras (2001a), The channel-hillslope integrated landscape development model (CHILD), in *Landscape Erosion and Evolution Modeling*, edited by R. S. Harmon and W. W. Doe, pp. 349–388, Springer, N. Y., USA.

Tucker, G. E., S. T. Lancaster, N. M. Gasparini, R. L. Bras, and S. M. Rybarczyk (2001b), An object-oriented framework for distributed hydrologic and geomorphic modeling using triangulated irregular networks, *Comp. Geosci.*, *27*(8), 959–973, doi:10.1016/S0098-3004(00)00134-5.

Valentin, C., J. Poesen, and Y. Li (2005), Gully erosion: Impacts, factors and control, *Catena*, *63*(2-3), 132–153, doi:10.1016/j.catena.2005.06.001.

Vandaele, K., J. Poesen, J. R. Marques Da Silva, and P. Desmet (1996), Rates and predictability of ephemeral gully erosion in two contrasting environments, *Geomorphol.: Relief, Processus, Environ.*, *2*, 83–96.

Vandekerckhove, L., J. Poesen, D. Oostwoud Wijdenes, and G. Gyssels (2001), Short-term bank gully retreat rates in Mediterranean environments, *Catena*, *44*(2), 133–161.

Vandekerckhove, L., J. Poesen, and G. Govers (2003), Medium-term gully headcut retreat rates in Southeast Spain determined from aerial photographs and ground measurements, *Catena*, *50*(2-4), 329–352, doi:10.1016/S0341-8162(02)00132-7.

Wahl, T. L. (1998), *Prediction of Embankment Dam Breach Parameters: A Literature Review and Needs Assessment*, DSO-98-004, pp. 59, Bureau of Reclamation, Water Resources Research Laboratory, Denver, CO, USA.

Wells, R. R., H. G. Momm, J. R. Rigby, S. J. Bennett, R. L. Bingner, and S. M. Dabney (2013), An empirical investigation of gully widening rates in upland concentrated flows, *Catena*, *101*, 114–121, doi:10.1016/j.catena.2012.10.004.

Whipple, K. X., and G. E. Tucker (1999), Dynamics of the stream-power river incision model: Implications for height limits of mountain ranges, landscape response timescales, and research needs, *J. Geophys. Res.*, *104*(B8), 17,661–17,674.

Wischmeier, W. H., and D. D. Smith (1978), *Predicting Rainfall Erosion Losses: A Guide to Conservation Planning*, USDA Agriculture Handbook no. 537, US. Govt. Printing Office, Washington, D. C., USA.

Wolf, P. R., and B. A. Dewitt (2000), *Elements of Photogrammetry With Applications in GIS*, 3rd ed., McGraw-Hill, New York USA.